

Supporting Information

Covalent Bridging of Corilagin Improves Antiferroptosis Activity: Comparison with 1,3,6- Tri-*O*-galloyl- β -D-glucopyranose

Xican Li,^{†,*} Jie Liu,[‡] Ban Chen,[†] Yingci Chen,[†] Wanjian Dai,[†] Yuling Li,[†]
and Meiling Zhu^{‡,§,*}

[†]School of Chinese Herbal Medicine, Guangzhou University of Chinese Medicine, Waihuan East Road No. 232, Guangzhou Higher Education Mega Center, Guangzhou, People's Republic of China, 510006.

[‡]Shenzhen Bao'an Traditional Chinese Medicine Hospital, Guangzhou University of Chinese Medicine, Shenzhen, People's Republic of China, 518101.

[§]Shenzhen Hospital of Integrated Traditional Chinese and Western Medicine, Shenzhen, People's Republic of China, 518101.

CONTENTS

Methods and Materials	S3
Figure S1. The certificate of analysis of corilagin.....	S7
Figure S2. The HPLC analysis of corilagin	S8
Figure S3. The MS spectra of corilagin.....	S9
Figure S4. The ¹ H-NMR of corilagin measured in CD ₃ OD.....	S10
Figure S5. The appearance of corilagin.....	S11
Figure S6. The certificate of analysis of TGG.....	S12
Figure S7. The HPLC analysis of TGG	S13
Figure S8. The MS spectra of TGG.....	S14
Figure S9. The ¹ H-NMR of TGG measured in CD ₃ OD	S15
Figure S10. The appearance of TGG.....	S16
Figure S11. Structures of some typical covalent-bridged egallotannins and their analogues.	S17
Figure S12. The does response curves of corilgin, TGG, and the positive control in Fe ²⁺ -chelating assay	S19
Figure S13. The does response curves of corilgin, TGG, and the positive control in PTIO [•] -inhibiting (pH 7.4) assay.....	S20
Figure S14. The does response curves of corilgin, TGG, and the positive control in PTIO [•] -inhibiting (pH 4.5) assay.....	S21
Figure S15. The does response curves of corilgin, TGG, and the positive control in Fe ³⁺ -reducing assay	S22
Figure S16. The does response curves of corilgin, TGG, and the positive control in DPPH [•] -inhibiting assay.....	S23
Table S1. The comparison of IC ₅₀ values of corilgin, TGG, and the positive control in five antioxidant assays.	S24

Methods and Materials

Animals, biological kits, and chemicals

Sprague-Dawley rats (4 weeks) were obtained from the Animal Centre of Guangzhou University of Chinese Medicine. The complete medium with glucose for SD rat bone marrow mesenchymal stem cells was purchased from Cyagen Biosciences (CA, USA); fetal bovine serum (FBS) and trypsin were from Molecular Probes (Carlsbad, USA). The probe C11-BODIPY was purchased from Molecular Probes (CA, USA). An annexin V/propidium iodide (PI) assay kit was purchased from *BD Biosciences* (NJ, USA). *Cell Counting Kit-8* kit was purchased from Dojindo Chemistry Research Institute (Kumamoto, Japan). Erastin was from MedChemExpress (Monmouth Junction, NJ, USA). Fetal bovine serum (FBS), rat bone mesenchymal stem cell Basal medium, and trypsin were purchased from Gibco (Grand Island, NY, USA). 4,4-Difluoro-5-(4-phenyl-1,3-butadienyl)-4-bora-3a,4a-diaza-s-indacene-3-undecanoic acid (C11-BODIPY) was obtained from Invitrogen (Carlsbad, CA, USA). Percoll was obtained from GE Healthcare Life Sciences (Pittsburgh, PA, USA). Trypsin was from Promega Co. (Madison, WI, USA). Ferrostatin-1 (Fer-1) was purchased from Selleck Chemicals (Houston, TX, USA).

Corilagin (C₂₇H₂₂O₁₈, CAS number: 23094-69-1, M.W. 634.5, purity 98%) and 1,3,6-tri-*O*-galloyl- β -D-glucopyranose (C₂₇H₂₄O₁₈, CAS number: 18483-17-5, M.W. 636.5, purity 98%) were obtained from Chengdu Biopurify Phytochemicals, Ltd. (Chengdu, China). The 3-(2-pyridyl)-5,6-bis(4-phenylsulfonic acid)-1,2,4-triazine (ferrozine) and (\pm)-6-hydroxyl-2,5,7,8-tetramethylchromane-2-carboxylic acid (Trolox) were obtained from Sigma-Aldrich (Shanghai, China). The 2-phenyl-4,4,5,5-tetramethylimidazoline-1-oxyl-3-oxide radical (PTIO^{*}) was from TCI Chemical Co. (Shanghai, China). 1,1-Diphenyl-2-picrylhydrazyl radical (DPPH^{*}, C₁₈H₁₂N₅O₆) was obtained from Aladdin Chemical, Ltd (Shanghai, China). Water and acetonitrile were of HPLC grade. FeCl₃·6H₂O and the other reagents of analytical grade were purchased from Guangdong Guanghua Chemical Plants Co., LTD (Shantou, China).

Extraction and culture of bone marrow-derived mesenchymal stem cells (bmMSCs)

The bmMSCs were extracted and cultured using our routine experimental protocols.¹ Briefly, male Sprague-Dawley rats were collected, and the adherent soft tissues were removed. Both ends of the bones were cut away from the diaphysis with bone scissors. The bone marrow plugs were hydrostatically expelled from the bones by insertion of needles fastened to 10-mL syringes filled with complete medium; the needles were inserted into the distal ends of femora and proximal ends of tibiae, and the marrow plugs expelled from the opposite ends. The cells were centrifuged and resuspended twice in complete medium; 5×10⁷ cells in 7-10 mL of complete medium were then introduced into 100-mm culture dishes. Two days later, the medium was changed and the nonadherent cells were discarded. The adherent cells were cultured in SD rat bone marrow mesenchymal stem cells complete medium with glucose, supplemented with 10 % (v/v) fetal bovine serum. The cultured cells were seeded and grouped to study the prevention of erastin-induced ferroptosis of corilagin and TGG.

Prevention of erastin-induced ferroptosis in bmMSCs

The erastin-induced ferroptosis model of bmMSCs was created based on the recent literature,² and with modifications. To measure the anti-ferroptosis bioactivities of corilagin and TGG, three assays referred as C11-BODIPY assay, flow cytometric assay, and CCK-8 assay.

The C11-BODIPY assay was used to characterize the degree of lipid peroxidation, and was performed using previously published method.³ Briefly, the cultured bmMSCs were seeded at 1×10^6 cells per well into 12-well plates. After adherence for 24 h, bmMSCs were divided into control, model, and sample groups. In the control group, bmMSCs were incubated for 12 h in Stel Basal medium. In the model and sample groups, bmMSCs were incubated in the presence of erastin (20 μM). After incubation for 12 h, the mixture of erastin and medium was removed. The bmMSCs in the model group were incubated for 12 h in Stel Basal medium, while BMSCs in the sample group were incubated for 12 h in Stel Basal medium with the indicated 3 $\mu\text{g}/\text{mL}$ sample concentrations and the positive control group with 1.0 μM Fer-1. The incubated cells were analyzed using the fluorescent probe C11-BODIPY (Invitrogen, Molecular Probes). Cells were incubated for 30 min prior to analysis with C11-BODIPY (2.5 μM). The images were taken using a fluorescence microscope.

The CCK-8 assay was conducted following previous literature,⁴ with minor modifications. Briefly, the cultured bmMSCs were seeded at 1×10^6 cells per well into 96-well plates. After adherence for 12 h, BMSCs were divided into control, model, positive control (Fer-1), and sample groups. The incubated cells were treated as above by adding 10 μL CCK-8, and the culture was incubated for an additional 3 h. The culture medium was discarded. Absorbance was measured at 450 nm on a Bio-Kinetics reader (Multiskan FC, Thermo Scientific, Shanghai, China). According to the $A_{450 \text{ nm}}$ values, the viability was calculated.

The flow cytometric assay was conducted according to the previous methods.⁵ Briefly, the cultured bmMSCs were seeded at 1×10^6 cells per well into 96-well plates. They were washed twice with cold PBS, and then resuspend cells in $1 \times$ Binding buffer at a concentration of 1×10^6 cells/mL. Then, 100 μL of the solution (1×10^5 cells) was transferred to a 5 mL culture tube, and 5 μL of FITC Annexin V and 5 μL PI were added. The cells were vortexed gently and were incubated for 15 min at room temperature in the dark, and 400 μL of $1 \times$ Binding Buffer was added to each tube after adherence for 12 h, BMSCs were divided into control, model, positive control (Fer-1), and sample groups. The three groups were analyzed by flow cytometry within 1 h. Each sample test was repeated in three independent wells.

Fe²⁺-chelation assays

The Fe²⁺-chealting activity of corilagin and TGG were preliminarily investigated using UV-vis spectra method.⁶ Briefly, 100 μL sample in methanol solution (3.17 mg/mL) and 100 μL FeCl₂•4H₂O aqueous solution (100 mg/mL) were added to 1800 μL of methanol-water (1:1, v/v), and mixed well. The resulting mixture was subsequently scanned using a UV-Vis spectrophotometer (Unico 2600A, Shanghai, China) from 400-900 nm in 30 min. Methanol/water (1:1, v/v) served as a blank. Next, 200 μL of the supernatant was transferred to a 96-well plate and photographed using a camera. The remaining solution were diluted and scanned from 200-400 nm.

Furthermore, the quantitative evaluation was conducted using a previously published method.⁷ Briefly, 0.05 mg/mL sample solution (30-150 μL) was added to a solution of 250 μM FeCl₂ (100 μL). The reaction was initiated by the addition of 500 μM ferrozine (150 μL). The total volume of the systems was adjusted to 1000 μL with methanol. Then, the mixture was shaken vigorously and left at room temperature for 5 min. Absorbance of the solution was then measured spectrophotometrically at 562 nm (Unico 2100, Shanghai, China). The percentage of Fe²⁺-chelation effect was calculated by using the formula given bellow:

$$\text{Fe}^{2+} \text{ - chelation \%} = \frac{A_0 - A}{A_0} \times 100\%$$

Where A is the absorbance in the presence of the sample or positive controls, while A_0 is the absorbance in the absence of the sample and positive controls.

PTIO•-scavenging assay

The PTIO•-scavenging assay was conducted based on our previously published method.⁸ Briefly, PTIO• radical was dissolved in phosphate buffers (pH 4.5 and 7.4) to prepare a PTIO• solution; the samples were prepared using methanol (2 mg/mL). Various volumes ($x = 2-10 \mu\text{L}$) of samples were mixed with phosphate buffers at pH 4.5 and 7.4 ($20 - x \mu\text{L}$) and treated with PTIO• solution (80 μL). After reaction at 37°C for 1 h, the product mixture was analyzed by measuring the absorbance at 560 nm on a microplate reader (Multiskan FC, Thermo Scientific, Shanghai, China). The PTIO• inhibition percentage was calculated as follows:

$$\text{Inhibition\%} = \frac{A_0 - A}{A_0} \times 100\%$$

Where A_0 is the absorbance value at 560 nm wavelength for the control sample (without test agent), and A is the absorbance value at 560 nm of the reaction mixture (with sample). The above experiment was repeated using phosphate buffers at different pH (including pH 4.5 and 7.4).

Fe³⁺-reducing antioxidant power (FRAP) assay

The FRAP assay was carried out as per the method described by Benzie,⁹ and slightly modified in our previous studies.¹⁰ Briefly, the FRAP reagent was freshly prepared by mixing 10 mM TPTZ, 20 mM FeCl₃, and 0.25 M acetate buffer (pH 3.6) at a ratio of 1:1:10. Samples (0.1 mg/mL, $x = 4-20 \mu\text{L}$) were added to ($20 - x$) μL of methanol and treated with 80 μL of FRAP reagent. After reaction for 30 min, the absorbance of the mixture was measured at 593 nm wavelength ($A_{593\text{nm}}$) on a microplate reader (Multiskan FC, Thermo Scientific, Shanghai, China). The relative reducing antioxidant power of the sample as compared to the maximum absorbance was calculated by the following formula:

$$\text{Relative reducing power\%} = \frac{A - A_{\min}}{A_{\max} - A_{\min}} \times 100\%$$

Where A_{\min} is the lowest $A_{593\text{nm}}$ value in the experiment, A is the $A_{593\text{nm}}$ value of the reaction mixture with sample, and A_{\max} is the greatest $A_{593\text{nm}}$ value in the experiment.

DPPH•-scavenging assay

The DPPH• radical scavenging activity was determined as previously described.¹¹ Briefly, 80 μL of DPPH•-methanolic solution (0.1 M) was mixed with sample-methanolic solution ($x = 1-5 \mu\text{L}$, 0.02 mg/mL) and ($20 - x$) μL methanol. The mixture was maintained at room temperature for 5 min, and the absorbance was measured at 519 nm on the microplate reader. The percentage of DPPH•-scavenging activity was calculated based on the formula presented for *PTIO•-scavenging assay*, wherein A_0 is the absorbance at 519 nm of the control and A is the absorbance at 519 nm of the test.

UHPLC-ESI-Q-TOF-MS analysis of DPPH• reaction products with corilagin and TGG

The reaction of DPPH• with corilagin and TGG proceeded under the conditions described in a previous method.¹² Briefly, a methanol solution of sample was mixed with a methanol DPPH• solution with a

molar ratio of 1:2, and the resulting mixture was kept for 24 h at room temperature. Subsequently, the product was passed through a 0.22- μm filter for UHPLC-ESI-Q-TOF-MS analysis.

The UHPLC-ESI-Q-TOF-MS analysis was based on the method described in our previous study.¹³ The UHPLC-ESI-Q-TOF-MS analysis system was equipped with a Phenomenex Luna C₁₈ column (2.1 mm i.d. \times 100 mm, 1.6 μm , Phenomenex Inc., Torrance, CA, USA). The mobile phase was employed for the elution of the system and consisted of a mixture of methanol (phase A) and 0.1% formic acid water (phase B). The column was eluted at a flow rate of 0.2 mL/min with the following gradient elution program: 0–2 min, maintained at 30% B; 2–10 min, 30–0% B; 10–12 min, 0–30% B. The sample injection volume was set at 3 μL for the separation of the different components. The Q-TOF-MS analysis was performed on a Triple TOF 5600^{plus} mass spectrometer (AB SCIEX, Framingham, MA, USA) equipped with an ESI source, which was run in the negative ionization mode. The scan range was set at 100–2000 Da. The system was run with the following parameters: ion spray voltage, –4500 V; ion source heater temperature, 550 °C; curtain gas pressure (CUR, N₂), 30 psi; nebulizing gas pressure (GS1, Air), 50 psi; Tis gas pressure (GS2, Air), 50 psi. The declustering potential (DP) was set at –100 V, whereas the collision energy (CE) was set at –45 V with a collision energy spread (CES) of 15 V.

Preferential conformation analysis by computational chemistry and molecular weight calculation

The preferential conformation was analyzed based on force fields by computational chemistry. Briefly, the energy minimization of both corilagin and TGG were, respectively, calculated through molecular mechanics II (MM2) using the Chem3D Pro14.0 program (PerkinElmer, Waltham, MA, USA). The preferential conformation has been expressed using the molecular models in **Figure 1C–D**. The Q-TOF-MS analysis is characterized by highly accurate m/z values, particularly molecular weights. The molecular weight calculation based on the formula is vital for comparison with the m/z values from the Q-TOF-MS analysis. In the present study, the molecular weight calculations of corilagin and TGG were conducted based on the accurate relative atomic masses. The relative atomic masses of C, H, O, and N were 12.0000, 1.007825, 15.994915, and 14.003074, respectively.

Statistical analysis

Each experiment was performed in triplicates; the data were recorded as mean \pm standard deviation (SD). The dose-response curves were plotted using Origin 2017 professional software (OriginLab, Northampton, MA, USA). The IC₅₀ value was defined as the final concentration of 50% radical inhibition (or relative reducing power). Statistical comparisons were carried out with one-way analysis of variance (ANOVA) to detect significant differences using SPSS 13.0 software (SPSS Inc., Chicago, IL, USA) for Windows. A value of $p < 0.05$ was considered statistically significant.

REFERENCES

1. Xie, H.; Li, X.; Ren, Z.; Qiu, W.; Chen, J.; Jiang, Q.; Chen, B.; Chen, D. Antioxidant and cytoprotective effects of Tibetan tea and its phenolic components. *Molecules* **2018**, *23* (2), 179.
2. Song, X.; Xie, Y.; Kang, R.; Hou, W.; Sun, X.; Epperly, M. W.; Greenberger, J. S.; Tang, D. FANCD2 protects against bone marrow injury from ferroptosis. *Biochem. Biophys. Res. Co.* **2016**, *480* (3), 443-449.
3. Aguirre, P.; García-Beltrán, O.; Tapia, V.; Muñoz, Y.; Cassels, B. K.; Núñez, M. T. Neuroprotective effect of a new 7, 8-dihydroxycoumarin-based Fe²⁺/Cu²⁺ chelator in cell and animal models of Parkinson's disease. *ACS Chem. Neurosci.* **2017**, *8* (1), 178-185.

4. Liu, J.; Li, X.; Cai, R.; Ren, Z.; Zhang, A.; Deng, F.; Chen, D. Simultaneous Study of Anti-Ferroptosis and Antioxidant Mechanisms of Butein and (*S*)-Butin. *Molecules* **2020**, *25* (3), 674.
5. Li, X.; Ren, Z.; Wu, Z.; Fu, Z.; Xie, H.; Deng, L.; Jiang, X.; Chen, D. Steric Effect of Antioxidant Diels-Alder-Type Adducts: A Comparison of Sanggenon C with Sanggenon D. *Molecules* **2018**, *23* (10), 2610.
6. Li, X.; Xie, Y.; Li, K.; Wu, A.; Xie, H.; Guo, Q.; Xue, P.; Maleshibek, Y.; Zhao, W.; Guo, J. Antioxidation and cytoprotection of acteoside and its derivatives: Comparison and mechanistic chemistry. *Molecules* **2018**, *23* (2), 498.
7. Ingold, K. U.; Pratt, D. A. Advances in radical-trapping antioxidant chemistry in the 21st century: a kinetics and mechanisms perspective. *Chem. Rev.* **2014**, *114* (18), 9022-9046.
8. Li, X. 2-Phenyl-4, 4, 5, 5-tetramethylimidazoline-1-oxyl 3-Oxide (PTIO[•]) Radical scavenging: A new and simple antioxidant assay *in vitro*. *J. Agr. Food Chem.* **2017**, *65* (30), 6288-6297.
9. Benzie, I. F.; Strain, J. J. The ferric reducing ability of plasma (FRAP) as a measure of "antioxidant power": the FRAP assay. *Anal. Biochem.* **1996**, *239* (1), 70-76.
10. Li, X.; Lin, J.; Chen, B.; Xie, H.; Chen, D. Antioxidant and cytoprotective effects of kukoamines A and B: Comparison and positional isomeric effect. *Molecules* **2018**, *23* (4), 973.
11. Li, X.; Jiang, Q.; Wang, T.; Liu, J.; Chen, D. Comparison of the antioxidant effects of quercitrin and isoquercitrin: Understanding the role of the 6''-OH group. *Molecules* **2016**, *21* (9), 1246.
12. Chen, B.; Li, X.; Liu, J.; Qin, W.; Liang, M.; Liu, Q.; Chen, D. Antioxidant and Cytoprotective effects of *Pyrola decorata* H. Andres and its five phenolic components. *BMC Complement. Altern. Med.* **2019**, *19* (1), 1-11.
13. Xie, Y.; Li, X.; Chen, J.; Deng, Y.; Lu, W.; Chen, D. pH effect and chemical mechanisms of antioxidant higenamine. *Molecules* **2018**, *23* (9), 2176.

Figure S1. The certificate of analysis of corilagin

产品分析证书
Certificate of Analysis

中文名称: 柯里拉京

English Name: Corilagin

别名(Alias):

产品编码(Cat. No.):BP0393

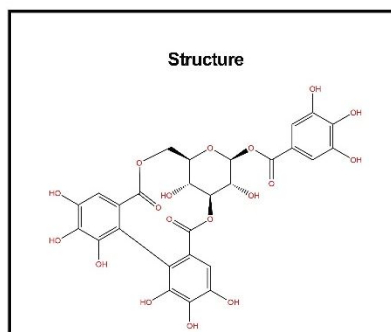
CAS Number: 23094-69-1

分子式(M. F.): C₂₇H₂₂O₁₈

分子量(M. W.): 634.455

批号(Batch No.): PRF7102406

报告日期(Report date): 2016/10/26



检验结果 (Analytical result) :

检验项目 (Test Item)	检验指标 (Specifications)	检验结果 (Results)
外观Appearance	Grey powder	Grey powder
干燥失重Loss on drying	<3.0%	1.34%
纯度Purity (HPLC-DAD, 276nm)*	≥98.0%	99.71%
质谱Mass	634.455±1	Conforms
核磁NMR	Comply with the structure	Conforms

* 色谱图见附件 (Please find HPLC chromatography attached.)

贮存条件 (Storage) :2~8℃

复测期 (Retest date) :two years (2018-10-25) under conditions list above.

备注 (Remarks) : 如遇质量问题, 请于收到产品之日起 15 日内与我们联系。

In case of quality issue, please contact us within 15 days after receipt of the product.

QC: Zhang Ling

Date: 2016年10月26日



QA: Wu Qi

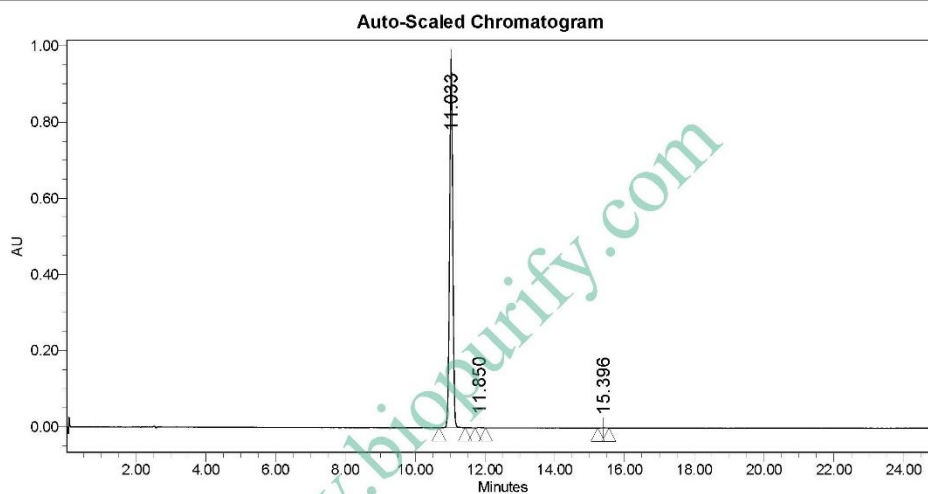
Date: 2016年10月26日

Tel: +86-28-82633987 Fax: +86-28-82633165

http://www.biopurify.com Email: sales@biopurify.com biopurify@gmail.com

Figure S2. The HPLC analysis of corilagin

SAMPLE INFORMATION			
Sample Name:	Corilagin PRF7102406	Acquired By:	System
Sample Type:	Unknown	Sample Set Name:	
Vial:	10	Acq. Method Set:	Corilagin
Injection #:	1	Processing Method:	Samples
Injection Volume:	10.00 ul	Channel Name:	276.0nm
Run Time:	25.0 Minutes	Proc. Chnl. Descr.:	PDA 276.0 nm
Date Acquired:	2016-10-25 9:27:08 CST		
Date Processed:	2016-10-25 10:02:41 CST		



Peak Results

Name	RT	Area	% Area	USP Plate Count	USP Resolution
1	11.033	6084641	99.71	70011.82	
2	11.850	7992	0.13	95774.42	4.67
3	15.396	9845	0.16	47331.14	15.93

Reported by User: System
 Report Method: Chengdu
 Report Method ID: 23197
 Page: 1 of 1

Project Name: 2016
 Date Printed:
 2016-10-25
 13:04:28 PRC

Figure S3. The MS spectra of corilagin

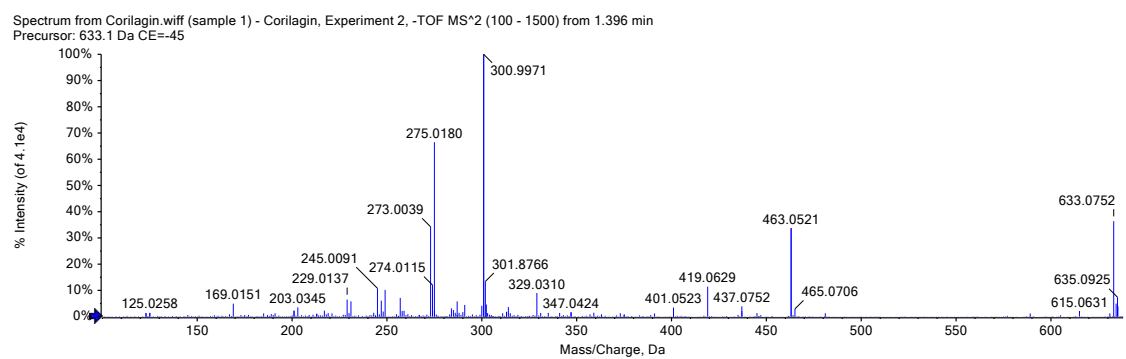
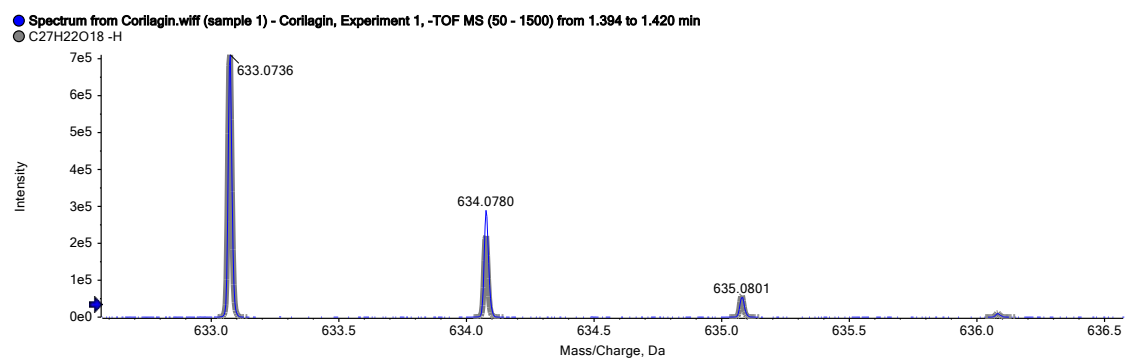
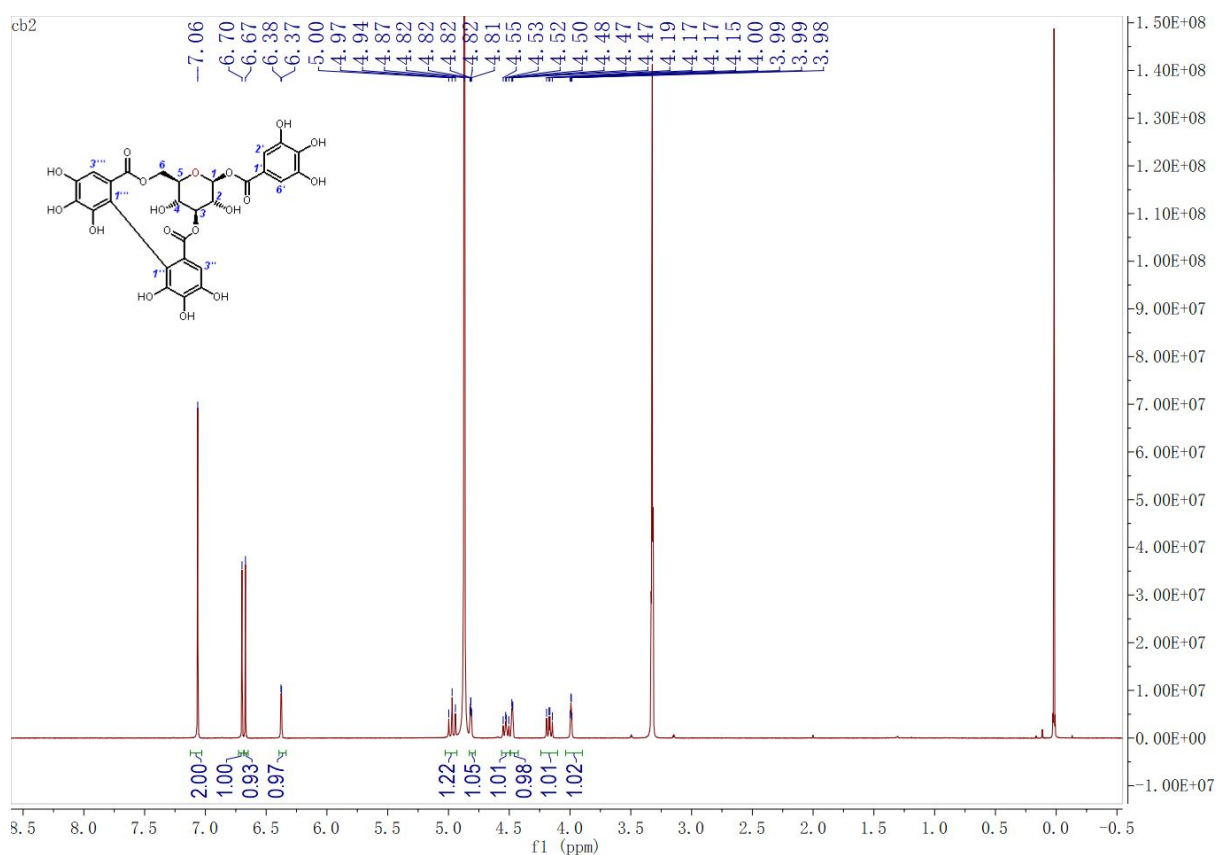


Figure S4. The $^1\text{H-NMR}$ of corilagin measured in CD_3OD



Corilagin $^1\text{H-NMR}$ (400 MHz, CD_3OD): δ 7.06 (s, 2H, H-2',6'), 6.70, 6.67 (each 1H, s, H-3'', H-3'''), 6.38 (d, J = 2.1 Hz, 1H, H-1), 4.97 (dd, J = 10.7, 8.1 Hz, 1H, H-6a), 4.83-4.78 (m, 1H, H-3), 4.53 (t, J = 10.9 Hz, 1H, H-5), 4.49-4.43 (m, 1H, H-4), 4.17 (dd, J = 11.0, 8.0 Hz, 1H, H-6b), 3.99 (dd, J = 3.6, 2.2 Hz, 1H, H-2).

Figure S5. The appearance of corilagin

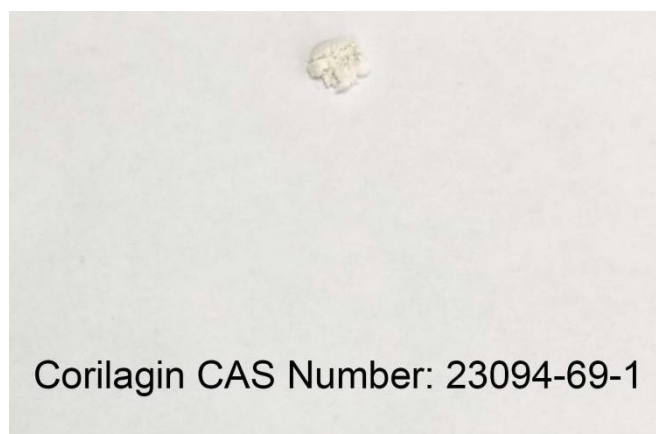


Figure S6. The certificate of analysis of TGG

产品分析证书
Certificate of Analysis

中文名称: 1,3,6-三-O-没食子酰葡萄糖

English Name: 1,3,6-Tri-O-galloyl-beta-D-glucose
别名 (Alias): 1,3,6-Tri-O-galloyl-beta-D-glucopyranose

产品编码 (Cat. No.): BP0004

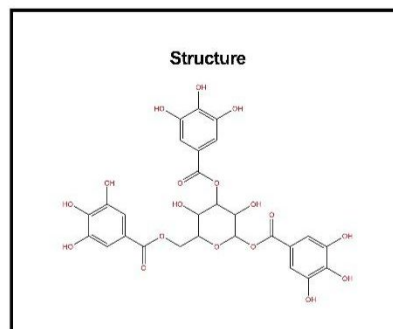
CAS Number: 18483-17-5

分子式 (M. F.): C₂₇H₂₄O₁₈

分子量 (M. W.): 636.471

批号 (Batch No.): PRF7093022

报告日期 (Report date): 2016/9/30



检验结果 (Analytical result) :

检验项目 (Test Item)	检验指标 (Specifications)	检验结果 (Results)
外观 Appearance	Light purple powder	Light purple powder
干燥失重 Loss on drying	<3.0%	1.07%
纯度 Purity (HPLC-DAD, 275nm)*	≥95.0%	95.55%
质谱 Mass	636.471±1	Conforms
核磁 NMR	Comply with the structure	Conforms

* 色谱图见附件 (Please find HPLC chromatography attached.)

贮存条件 (Storage) : 2~8℃

复测期 (Retest date) : two years (2018-09-29) under conditions list above.

备注 (Remarks) : 如遇质量问题, 请于收到产品之日起 15 日内与我们联系。

In case of quality issue, please contact us within 15 days after receipt of the product.

QC: Zhang Ling
Date: 2016年9月30日



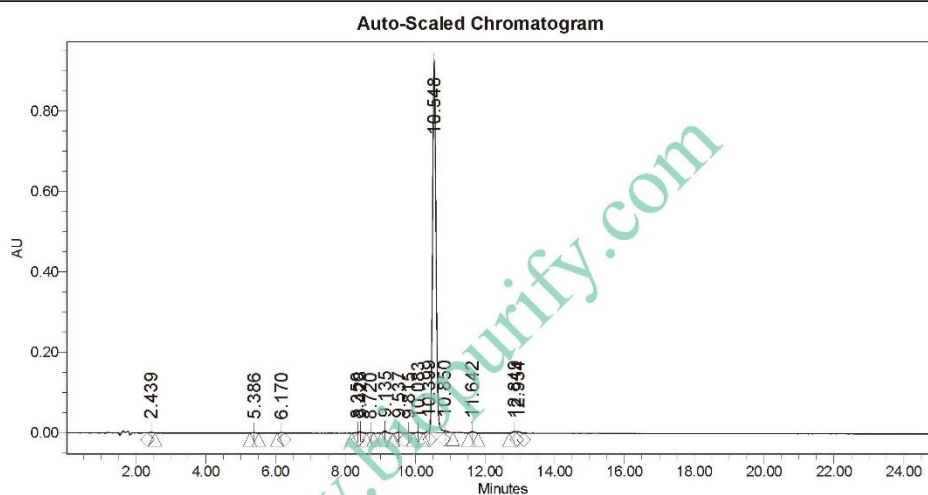
QA: Wu Qi
Date: 2016年9月30日

Tel: +86-28-82633987 Fax: +86-28-82633165

http://www.biopurify.com Email: saks@biopurify.com biopurify@gmail.com

Figure S7. The HPLC analysis of TGG

SAMPLE INFORMATION			
Sample Name:	PRF7093022	Acquired By:	System
Sample Type:	Unknown	Sample Set Name:	
Vial:	93	Acq. Method Set:	1 3 6 Tri O galloyl beta D glu
Injection #:	1	Processing Method:	Samples
Injection Volume:	5.00 ul	Channel Name:	275.0nm
Run Time:	25.0 Minutes	Proc. Chnl. Descr.:	PDA 275.0 nm
Date Acquired:	2016-9-30 11:35:21 CST		
Date Processed:	2016-9-30 12:36:44 CST		



Peak Results

Name	RT	Area	% Area	USP Plate Count	USP Resolution
1	2.439	10452	0.16	5636.74	
2	5.386	6454	0.10	6519.90	19.03
3	6.170	5950	0.09	14779.06	4.35
4	8.350	6918	0.11		11.80
5	8.428	25852	0.39	28307.99	0.36
6	8.720	7404	0.11	22694.74	1.34
7	9.135	38058	0.58	41665.84	2.28
8	9.537	27457	0.42	38078.34	2.18
9	9.815	11659	0.18	59778.49	1.55
10	10.083	14569	0.22	49948.42	1.54
11	10.399	29722	0.45		1.75

Reported by User: System
 Report Method: Chengdu
 Report Method ID: 21932
 Page: 1 of 2

Project Name: 2016
 Date Printed:
 2016-9-30
 12:45:21 PRC

Figure S8. The MS spectra of TGG

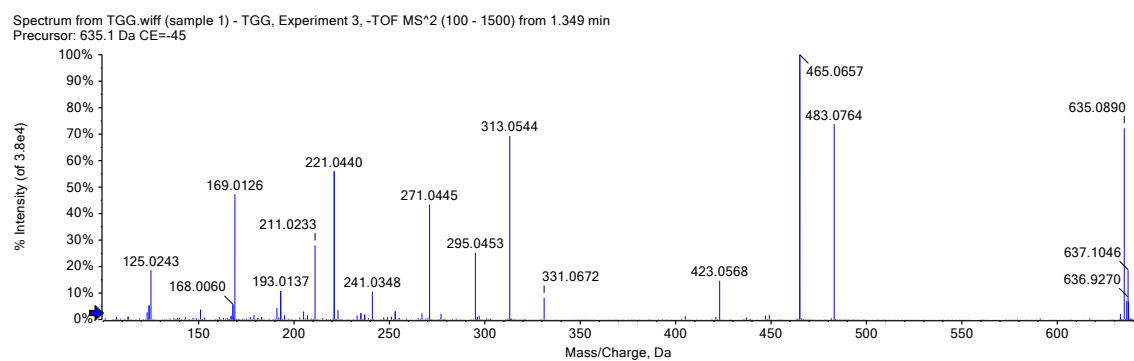
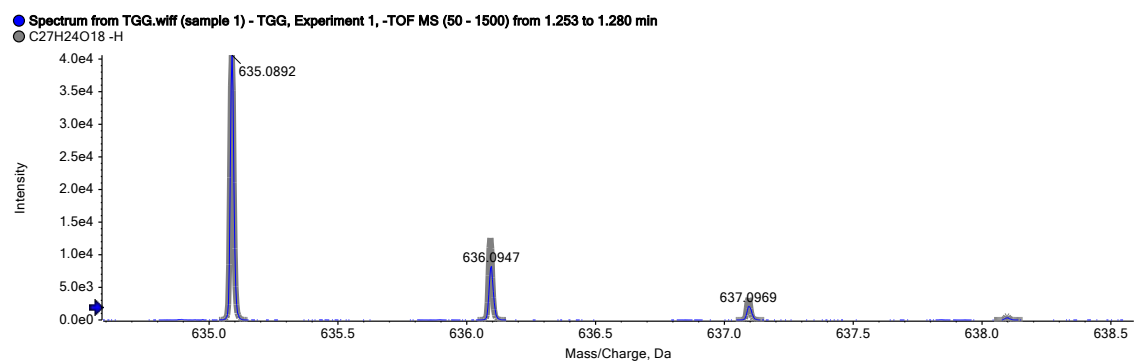
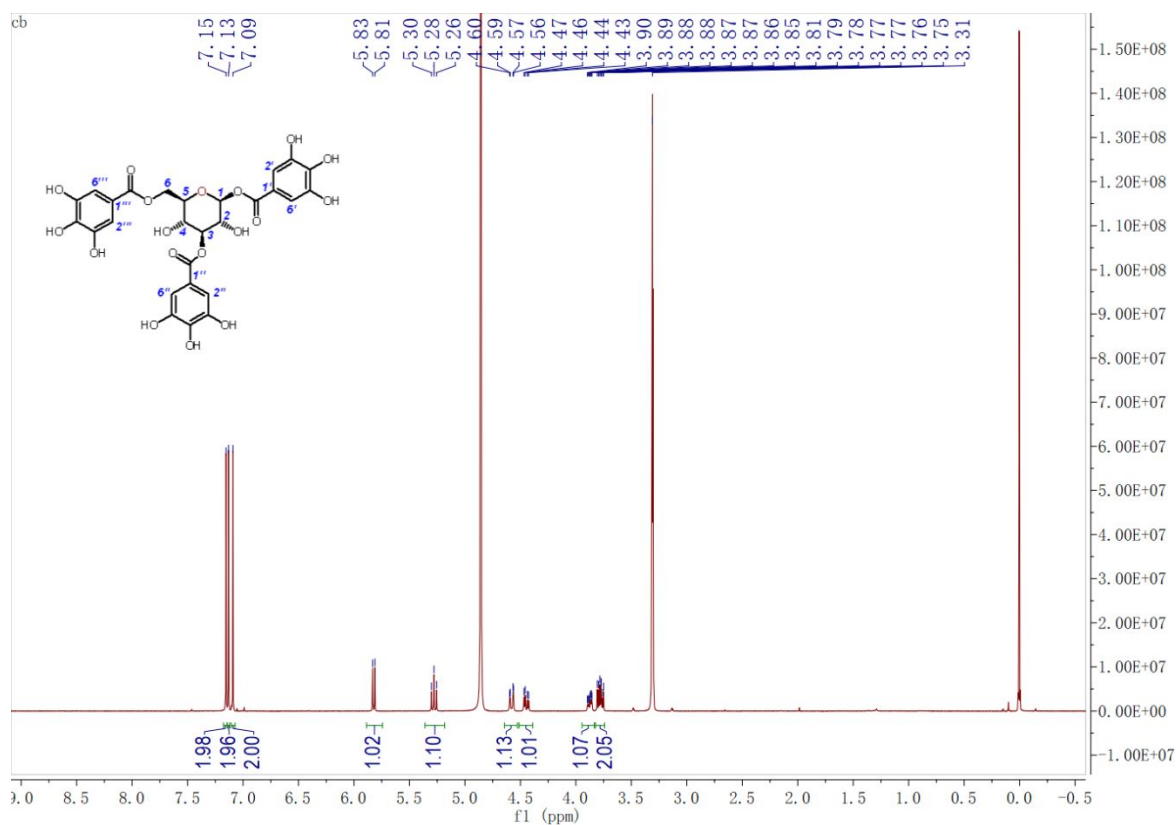


Figure S9. The $^1\text{H-NMR}$ of TGG measured in CD_3OD



TGG $^1\text{H NMR}$ (400 MHz, CD_3OD): δ 7.15 (s, 2H, H-2',6'), 7.13 (s, 2H, H-2'',6''), 7.09 (s, 2H, H-2''',6'''), 5.82 (d, $J = 8.2$ Hz, 1H, H-1), 5.28 (t, $J = 9.3$ Hz, 1H, H-3), 4.58 (dd, $J = 12.1, 1.9$ Hz, 1H, H-6a), 4.45 (dd, $J = 12.2, 4.8$ Hz, 1H, H-6b), 3.88 (ddd, $J = 9.8, 4.7, 1.9$ Hz, 1H, H-5), 3.82 – 3.74 (m, 2H, H-2,4).

Figure S10. The appearance of TGG

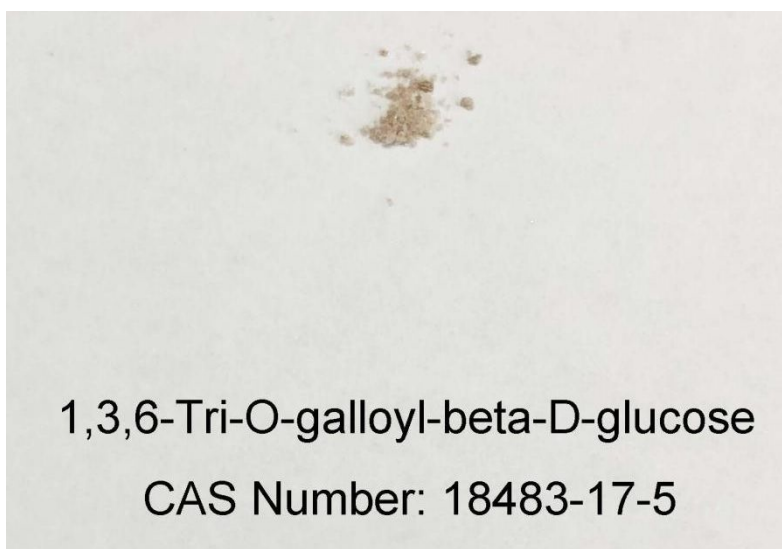
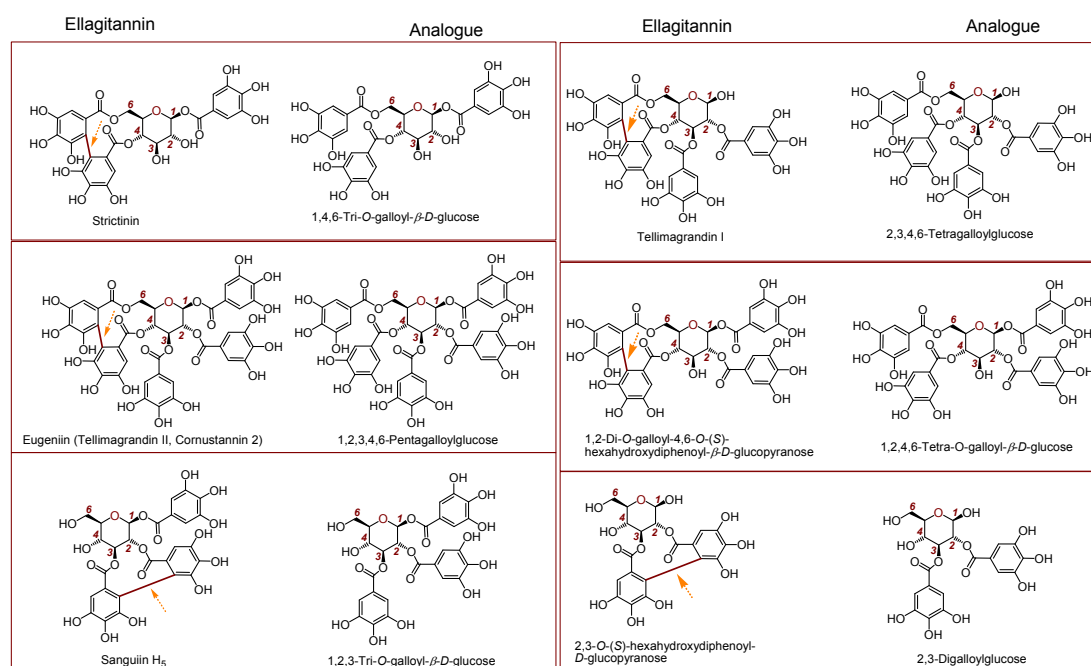


Figure S11. Structures of some typical covalent-bridged ellagitannins and their analogues.



Eugeniiin¹ vs 1,2,3,4,6-pentagalloylglucose²; tellimagrandin I³ vs 2,3,4,6-tetragalloylglucose⁴; sanguiniin H₅⁵ vs 1,2,3-tri-O-galloyl-β-D-glucose⁶; 1,2-di-O-galloyl-4,6-O-(S)-hexahydroxydiphenoyl-β-D-glucopyranose⁷ vs 1,2,4,6-tetra-O-galloyl-β-D-glucose⁸; strictinin⁹ vs 1,4,6-tri-O-galloyl-β-D-glucose¹⁰; 2,3-O-(S)-hexahydroxydiphenoyl-D-glucopyranose⁷ vs 2,3-digalloylglucose¹¹.

REFERENCES

1. Nonaka, G.-I.; Harada, M.; Nishioka, I. J. C.; Bulletin, P. Eugeniiin, a new ellagitannin from cloves. *Chem. Pharm. Bull.* **1980**, *28* (2), 685-687.
2. Abdelwahed, A.; Bouhlel, I.; Skandrani, I.; Valenti, K.; Kadri, M.; Guiraud, P.; Steiman, R.; Mariotte, A.-M.; Ghedira, K.; Laporte, F. J. Study of antimutagenic and antioxidant activities of Gallic acid and 1, 2, 3, 4, 6-pentagalloylglucose from *Pistacia lentiscus*: Confirmation by microarray expression profiling. *Chem.-Biol. Interact.* **2007**, *165* (1), 1-13.
3. Shiota, S.; Shimizu, M.; Mizusima, T.; Ito, H.; Hatano, T.; Yoshida, T.; Tsuchiya, T. J. Restoration of effectiveness of β-lactams on methicillin-resistant *Staphylococcus aureus* by tellimagrandin I from rose red. *FEMS Microbiol. Lett.* **2000**, *185* (2), 135-138.
4. Yin, T.-P.; Cai, L.; Chen, Y.; Li, Y.; Wang, Y.-R.; Liu, C.-S.; Ding, Z.-T. Tannins and antioxidant activities of the walnut (*Juglans regia*) pellicle. *Nat. Prod. Commun.* **2015**, *10* (12), 1934578X1501001232.
5. Natangelo, A. Towards the first total synthesis of C-arylglucosidic ellagitannins. A biomimetic approach. *Pubblicazioni dello IUSS* **2009**, *3* (1), 1-235.
6. Lee, J.; Jang, D. S.; Kim, N. H.; Lee, Y. M.; Kim, J.; Kim, J. S. J. B.; Bulletin, P. Galloyl glucoses from the seeds of *Cornus officinalis* with inhibitory activity against protein glycation, aldose reductase, and cataractogenesis ex vivo. *Biol. Pharm. Bull.* **2011**, *34* (3), 443-446.
7. Fukuda, T.; Ito, H.; Yoshida, T. Antioxidative polyphenols from walnuts (*Juglans regia* L.). *Phytochemistry* **2003**, *63* (7), 795-801.
8. Si, C.; Zhang, Y.; Zhu, Z.; Liu, S. Chemical constituents with antioxidant activity from the pericarps of *Juglans sigillata*. *Chem. Nat. Compd.* **2011**, *47* (3), 442.

9. Chen, G.-H.; Lin, Y.-L.; Hsu, W.-L.; Hsieh, S.-K.; Tzen, J. Significant elevation of antiviral activity of strictinin from Pu'er tea after thermal degradation to ellagic acid and gallic acid. *J. Food Drug Anal.* **2015**, *23* (1), 116-123.
10. Kolodziej, H.; Kayser, O.; Kiderlen, A.; Ito, H.; Hatano, T.; Yoshida, T.; Foo, L. Antileishmanial activity of hydrolyzable tannins and their modulatory effects on nitric oxide and tumour necrosis factor- α release in macrophages in vitro. *Planta Med.* **2001**, *67* (09), 825-832.
11. Nakashima, H.; Murakami, T.; Yamamoto, N.; Sakagami, H.; Tanuma, S.-i.; Hatano, T.; Yoshida, T.; Okuda, T. Inhibition of human immunodeficiency viral replication by tannins and related compounds. *Antiviral Res.* **1992**, *18* (1), 91-103.

Figure S12. The does response curves of corilgin, TGG, and the positive control in Fe²⁺-chelating assay

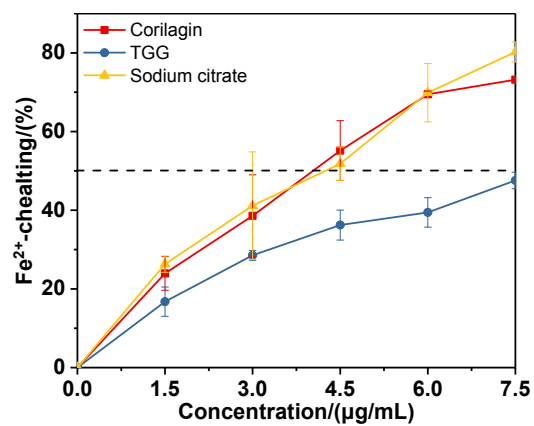


Figure S13. The does response curves of corilgin, TGG, and the positive control in PTIO-inhibiting (pH 7.4) assay

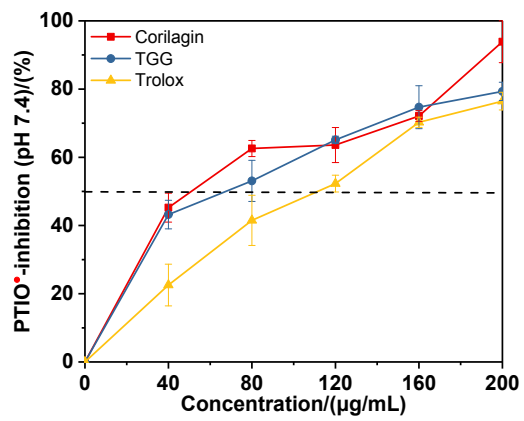


Figure S14. The does response curves of corilagin, TGG, and the positive control in PTIO[•]-inhibiting (pH 4.5) assay

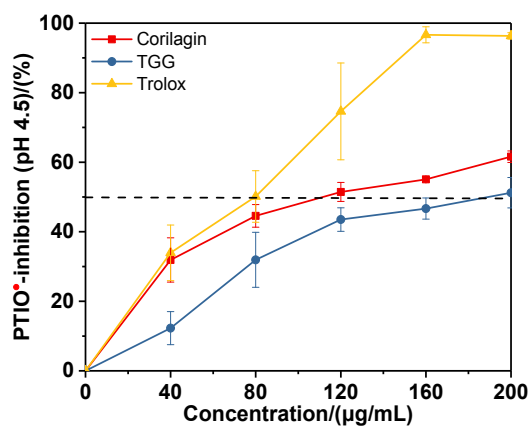


Figure S15. The does response curves of corilagin, TGG, and the positive control in Fe³⁺-reducing assay

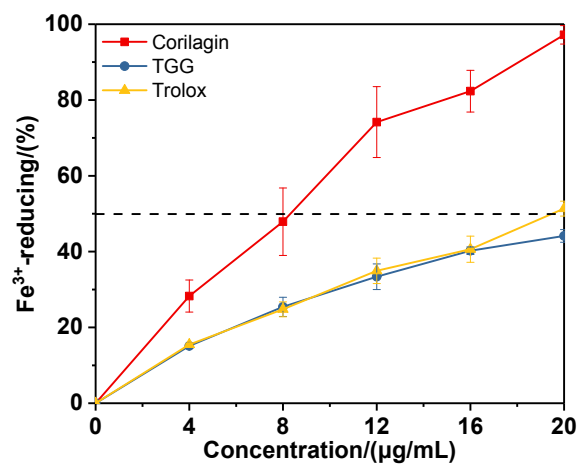


Figure S16. The does response curves of corilagin, TGG, and the positive control in DPPH[•]-inhibiting assay

